

Photovoltaic Solar Electrochemical Oxidation (PSEO) for lignosulfonate waste water treatment

Antonio Dominguez-Ramos, Rubén Aldaco, Angel Irabien*

Department of Chemical Engineering and Inorganic Chemistry, University of Cantabria
Avda. Los Castros, s.n., Santander, Spain
irabienj@unican

Under the current global energy scenario, the need of self-sustainable processes is encouraged. A process of Photovoltaic Solar powered Electrochemical Oxidation (PSEO) has been developed to remove the organic matter from lignosulfonate waste water. Experimental results show that the process is able to oxidize the organic matter up to removal yields around 90% of Total Organic Carbon (TOC) under the described operating conditions, demonstrating the technical suitability of the PSEO process.

1. Introduction

Electrochemical oxidation has been pointed out as very promising option for waste water treatment due to several attractive features: no need of chemicals, zero production of sludge, easy control and automation... However, the high specific energy consumption (Cañizares et al., 2002) when compared with conventional processes such as activated sludge still remains as a serious handicap for this electrochemical technology. Therefore, innovative self sustainable processes through Process Integration should help at overcoming the current global bounded problems of fossil fuels dependence and water scarcity. In order to overcome the current handicap of the electrochemical oxidation, a novel process called Photovoltaic Solar Electrochemical Oxidation (PSEO) was developed, in which an electrochemical reactor is coupled to a set of photovoltaic solar modules.

The aim of this work is therefore the demonstration of the technical suitability of a Photovoltaic Solar Electrochemical Oxidation (PSEO) process to degrade the organic matter from a lignosulfonate synthetic solution.

2. Materials & Methods

In order to check the reliability of the PSEO process, a synthetic solution of lignosulfonate was used as a reference of biorefractory organic matter. A commercial Borrebond 55S calcium-magnesium lignosulfonate from *Eucalyptus globulus* (sulfite process) was used as a base for the solutions. Synthetic solutions were treated in an electrochemical reactor (Adamant Technologies SA) using Boron Doped Diamond electrodes and operating in a batch mode. A scheme of the experimental setup is shown in Figure 1.

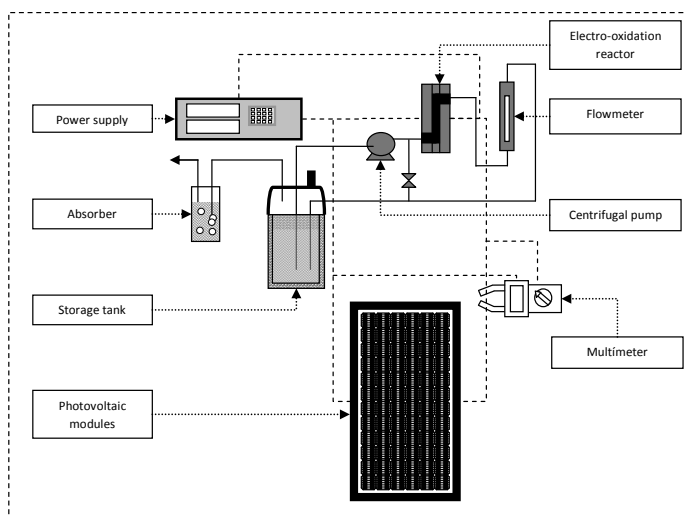


Figure 1. Scheme of the experimental set up.

Anode and cathode are both circular with a total wet area (A_E) of 70 cm^2 per electrode (inter-electrode gap of 1 mm). A centrifugal pump was used to circulate the solution through the electrochemical cell. The PSEO process lab-scale plant is based on four monocrystalline photovoltaic modules (SunTech Co. Ltd. STP160) for a total peak power of 640 W_p . Photovoltaic modules were placed on the roof of ETSIIyT, University of Cantabria, Santander, Spain ($W3^\circ47'52.17''$, $N43^\circ28'22.33''$) tilted at 38° and south orientation (20° West). The set of modules were directly connected to the electrochemical reactor through a fuse box.

Table 1. Experimental conditions

Exp	Date	Number of PV modules	t_{OP}	C_0	$[\text{Na}_2\text{SO}_4]$
			min	$\text{mgC}\cdot\text{L}^{-1}$	$\text{g}\cdot\text{L}^{-1}$
E1	29-04-2008	2	300	624	2.5
E2	05-05-2008	4	240	700	2.5
E3	07-05-2008	2	300	200	2.5
E4	15-05-2008	1	480	656	0.3

Total Organic Carbon (TOC) of each sample was analyzed using a Shimadzu TOC-V CPH with ASI-V operating with synthetic air from Air Liquide SA, (pressure: 200 KPa ; flowrate: $150 \text{ mL}\cdot\text{min}^{-1}$). A Hach HQ40d unit (Hach Lange) was used to measure pH and conductivity. Solar irradiance time profiles were measured at intervals of 15 minutes using a SunReader unit (SunTechnics Conergy Group). To obtain current, voltage and power time profiles a Fluke 345 unit was used for measurements and recordings. Table 1 summarizes relevant operating conditions in the experiments. The local initial time for experiments was 10:30 PM. The operation time t_{OP} was extended to keep a TOC removal around 90%. Flow-rate through the electrochemical cell was kept constant at $300 \text{ L}\cdot\text{h}^{-1}$. The temperature of the solution was maintained constant between

22-24 °C for the selected experiments (except for E2 at 32 °C). Samples were withdrawn from the solution tank at regular times.

3. Results and discussion

Figure 2 shows the time profiles for incident solar power g (solar irradiance on the plane defined by the position of the photovoltaic modules G multiplied by the corresponding effective module area A_M) and the total output current i (inset of Figure 2).

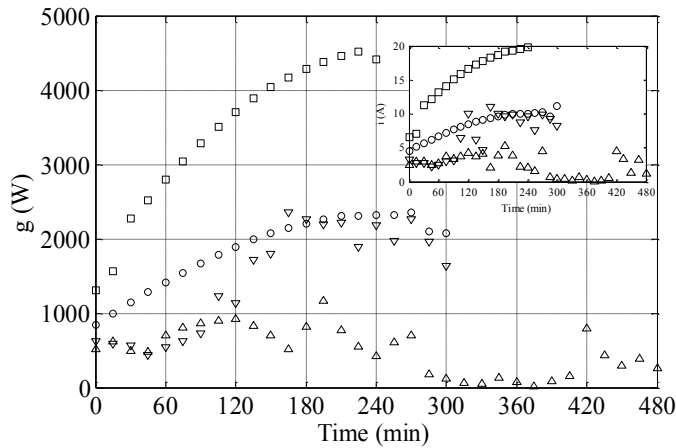


Figure 2. Incident solar power $g=GA_M$ versus time. E1. (○) E1; (□) E2; (◇) E3; (△) E4. Inset: evolution of total applied current i versus time. (○) E1; (□) E2; (◇) E3; (△) E4.

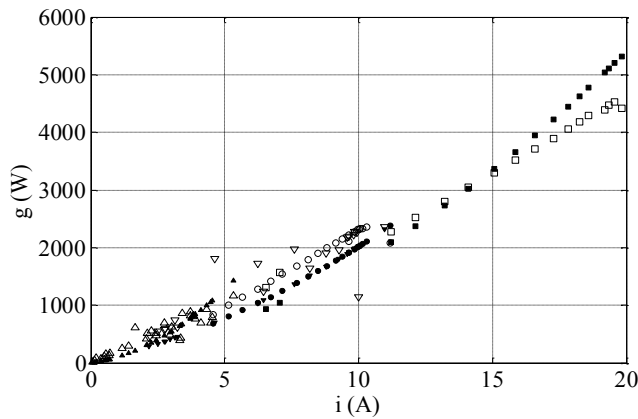


Figure 3. Incident solar power g versus total applied current i for experiments (○) E1; (□) E2; (◇) E3; (△) E4 and calculated values (●) E1; (■) E2; (◆) E3; (▲) E4.

The maximum experimental value of g was 4.53 kW and 19.8 A for i respectively. It is remarkable that the higher values of g were obtained for the experiment E2 which was operating under clear sky conditions and the maximum number of photovoltaic modules connected in parallel. On the contrary, lower values of g were obtained for E4, when only one photovoltaic module was connected and clouds appear during the experiment. To check the experimental results, the maximum irradiance under clear sky conditions was used as reference. From the Photovoltaic Geographical Information System (PVGIS) of the JRC of the European Commission (Joint Research Center of the European Commission <re.jrc.ec.europa.eu/pvgis> accessed in 2009), a maximum daily value of global clear sky solar irradiance of $981 \text{ W}\cdot\text{m}^{-2}$ was obtained for May (tilt of 38° and south orientation 20° W) in Santander, so the theoretical maximum value of g was 4.42 kW.

$$g = \frac{p}{\eta} = \frac{iv}{\eta} = \frac{i(v_0 + iR)}{\eta} = \frac{iv_0 + i^2R}{\eta} \begin{cases} g \approx \frac{v_0}{\eta}i \text{ for low } i \text{ values} \\ g \approx \frac{R}{\eta}i^2 \text{ for high } i \text{ values} \end{cases} \quad (1)$$

Figure 3 shows a linear relationship for low values of g and a positive deviation as g increases. Consequently, there is a relationship between those variables that should consider the fact that at high g values the relationship is no longer linear. Assuming that η is the module efficiency, v_0 is the voltage required to generate a faradaic current and R the total ohmic resistance, a relationship is shown in eq. 1. Black dots in Figure 3 show predicted values and a good agreement is observed.

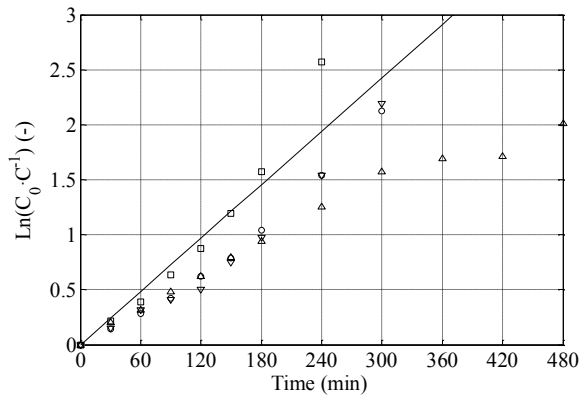


Figure 4. Organic matter removal with time for experiments (○) E1; (□) E2; (◇) E3; (△) E4. (-) K-line.

TOC removal (expressed as the logarithm of C_0/C) with time is shown in Figure 4. The maximum theoretical TOC removal rate is shown in Figure 4 as a line with zero crossing named K-line, whose slope is based on the maximum observed kinetic constant $K_{\max} = 8.09 \cdot 10^{-3} \text{ min}^{-1}$ reported previously for the experimental setup under laboratory controlled current conditions (Dominguez Ramos et al., 2008). It is expected that all

experimental points were below the K-line as long as no other oxidation mechanism is involved. A maximum value of $K_m=2.31 \cdot 10^{-3} \text{ m} \cdot \text{min}^{-1}$ from previous laboratory studies was obtained, which is used as reference. The observed kinetic constant K_{exp} and corresponding standard error (at 95% confidence level) for each experiment according to a first order kinetic is reported in Table 2. To compare experiments, an average input current i_p and solar power g_p were defined for each experiment.

From Figure 4, a removal close to 90% is obtained for both experiments E2 and E4 at a different number of hours of operation. It is observed from Figure 4 that experimental values for E2 are in the reference K-line during the first three hours of operation. After three hours, a deviation of experimental values above the K-line is observed for the two last experimental points. This deviation (only observed in E2) corresponds with the highest value of the average input current $i_p=15.39 \text{ A}$ and the higher value of the kinetic constant $K_{\text{exp}}=2.28 \cdot 10^{-3} \text{ m} \cdot \text{min}^{-1}$. It has been suggested an additional mechanism to the electrochemical oxidation with hydroxyl radicals, which could be used to explain the behavior for the whole set of four experiments.

Table 2. Apparent kinetic constants and specific energy consumption

Exp	i_p A	g_p kW	$K_{\text{exp}} \cdot 10^3$ $\text{m} \cdot \text{min}^{-1}$	$E_{\text{SC,m}}$ $\text{kWh} \cdot \text{kgC}^{-1}$	$E_{\text{SC,v}}$ $\text{kWh} \cdot \text{m}^{-3}$
E1	8.48	1.86	1.80 ± 0.18	534	294
E2	15.39	3.43	2.28 ± 0.20	882	571
E3	6.69	1.47	1.79 ± 0.24	1035	184
E4	2.42	0.50	1.31 ± 0.09	176	100

This mechanism assumes that two serial steps could be taking place: i) the direct oxidation by hydroxyl radicals OH^\cdot in the close layer of liquid surface of the electrode ii) the mass transfer of organic matter from the bulk to the electrode surface. Consequently, if the reaction rate in the close layer of liquid of the electrode is fast enough, the process will be mass transfer controlled. Additionally, the indirect oxidation by electro-generated reagents (peroxodisulfates if sodium sulfate is used), whose concentration in the bulk phase depends on the applied current and for which there is no mass transfer limitations (Michaud et al., 2000; Serrano et al., 2002) could be contributing in a parallel way. At these values of applied current ($i_p = 15.39 \text{ A}$), the contribution of the parallel reaction by electro-generated oxidants is suggested to have a certain extension, making the reaction rate to be higher than those obtained for lower values so a maximum concentration of electro-generated peroxodisulfates was expected. If this additional mechanism is considered and assuming that the higher the applied current the higher is the concentration of oxidants in the bulk phase, an increase in the applied current may lead to reaction rates over the theoretical maximum reaction rate, which only considers the two serial steps mechanism: oxidation by hydroxyl radicals at the close layer of the electrode surface and mass transfer from the bulk phase to the electrode surface. In E4, the lower values of the input current did take place ($i_p=2.42 \text{ A}$) and the kinetic constant $K_{\text{exp}}=1.31 \cdot 10^{-3} \text{ m} \cdot \text{min}^{-1}$ was also the lower constant. Therefore, it was expected that the extension of parallel reactions of electro-generated reagents was negligible in E4, in which the applied current had the lower values. Despite having

different solar irradiance profiles and initial concentrations but similar average input currents, from Figure 4 it can be deduced that it is possible to achieve up to 90% in TOC removal for E1 and E3 as well as in E2 and E4 but for similar t_{OP} . Considering the K-line in Figure 4, it is observed that the experimental degradation rate is below the maximum rate in both experiments ($K_{exp}=1.80\cdot 10^{-3}$ - $1.79\cdot 10^{-3}$ m \cdot min $^{-1}$ respectively for E1 and E3) for the whole considered experimental time.

Table 2 shows the specific values of energy consumption. From Table 2, it can be seen that the lowest value comes from E4 (100 kWh \cdot m $^{-3}$), which corresponds to the lower mean irradiation. The consumption of energy was shown to be higher than for controlled current conditions (Dominguez-Ramos et al., 2008), which means that the ratio between the electrode area and the module area can be largely optimized for an effluent with fixed characteristics. Optimization of this ratio helps at preventing an excess of applied current and therefore to allow the process to perform in a sustainable way due to an appropriate investment economic cost and a friendly environmental profile.

4. Conclusions

The PSEO technical suitability was demonstrated considering the obtained removal rates. Additionally, the PSEO process performance was discovered to be dependant of the applied current, being a linear relationship between the solar irradiation and the output current under when low current values were obtained. Taking into consideration the specific energy consumption, the ratio between the electrode area and the module area can be largely optimized for an effluent with fixed characteristics.

References

- Cañizares P., Díaz M., Domínguez J.A. and García-Gómez J., Rodrigo M.A., 2002, Electrochemical oxidation of aqueous phenol wastes on synthetic diamond thin-film electrodes. *Ind. Eng. Chem. Res.* 41, 4187-4194.
- Dominguez-Ramos A., Aldaco R. and Irabien A., 2008, Electrochemical Oxidation of Lignosulphonate: Total Organic Carbon Oxidation Kinetics. *Ind. Eng. Chem. Res.* 47(24), 9848-9853.
- Serrano K., Michaud P.A., Comminellis C. and Savall A., 2002, Electrochemical preparation of peroxodisulfuric acid using boron doped diamond thin film electrodes. *Electrochim. Acta* 48, 431-6.
- Michaud P., Mahé E., Haenni W., Perret A. and Comminellis C., 2000, Preparation of peroxodisulfuric acid using boron-doped diamond thin film electrodes. *Electrochem. Solid-State Lett.* 3, 77-9.